Available online at www.sciencedirect.com
ScienceDirect
Ceramics International 37 (2011) 2377–2382
CERAMICS INTERNATIONAL
www.elsevier.com/locate/ceramint

Low-temperature sintering and microwave dielectric properties of 3Z2B glass–Al_2O_3 composites

Dong-Xiang Zhou [a,b], Rong-Guang Sun [a], Shu-Ping Gong [a], Yun-Xiang Hu [a,*]

[a] Department of Electronic Science and Technology, Huazhong University of Science and Technology, Wuhan 430074, China
[b] State Key Laboratory of Material Processing and Die & Mould Technology, Huazhong University of Science and Technology, Wuhan 430074, China

Received 3 March 2011; accepted 21 March 2011
Available online 29 March 2011

Abstract

A potential low temperature co-fired ceramics system based on zinc borate $3ZnO–2B_2O_3$ (3Z2B) glass matrix and Al_2O_3 filler was investigated with regard to phase development and microwave dielectric properties as functions of the glass content and sintering temperature. The densification mechanism for 3Z2B–Al_2O_3 composites was reported. The linear shrinkage of 3Z2B glass–Al_2O_3 composites exhibited a typical one-stage densification behavior. XRD patterns showed that a new crystalline phase, $ZnAl_2O_4$ spinel, formed during densification, indicating that certain chemical reaction took place between the 3Z2B glass matrix and the alumina filler. Meanwhile, several zinc borate phases, including $4ZnO{\cdot}3B_2O_3$, crystallized from the glass matrix. Both of the reaction product phase and crystallization phases played an important role in improving the microwave dielectric properties of composites. The optimal composition sintered at 850–950 °C showed excellent microwave dielectric properties: $\varepsilon_r = \sim 5.0$, $Q{\cdot}f_0 = \sim 8000$ GHz, and $\tau_f = \sim -32$ ppm/°C at ~7.0 GHz.

Keywords: A. Sintering; B. X-ray methods; C. Dielectric properties

1. Introduction

Small, light weight and multifunctional electronic components are attracting much attention because of the rapid growth of the wireless communication systems and microwave products in the consumer electronic market. The component manufacturers are thus forced to search for new advanced integration, packaging, and interconnection technologies. One solution is the low temperature co-fired ceramics (LTCC) technology enabling fabrication of three-dimensional ceramic modules with the low dielectric loss and embedded Ag, Cu, Au, etc. electrodes [1]. The substrate material is one of the most important constituents of LTCC. The key characteristics required for a substrate material are: (i) low dielectric constant ($\varepsilon_r < 10$, to increase the signal speed), (ii) low dielectric loss or high quality factor (to increase selectivity), (iii) high thermal conductivity (to dissipate the heat generated), (iv) low or matching coefficient of thermal expansion (CTE) to that of the materials attached to it, and (v) low temperature coefficient of resonant frequency, τ_f [2–7]. In general, there are two main methods to lower the sintering temperature of ceramics. The first approach is via the glass–ceramic route, which starts with a fully glassy system that devitrifies almost completely during the sintering process. A good example is Ferro A6M containing $CaO–SiO_2–B_2O_3$ glass which forms wollastonite ($CaSiO_3$) during firing. In the second approach (glass + ceramic), the starting material consists of a low softening point glass and a crystalline ceramic. Typical systems with this approach include the borosilicate glass (BSG) + alumina by Fujitsu and the lead BSG + alumina by DuPont.

Alumina, which exhibits good dielectric properties ($\varepsilon_r = 10.5$, unloaded quality factor $Q{\cdot}f_0 = 680{,}000$ GHz, and $\tau_f = -60$ ppm/°C), is widely used as a ceramic filler of substrate materials at high frequencies [8]. Seo et al. [9] reported that compositions of $La_2O_3–B_2O_3$ glass filled with different amounts of Al_2O_3 exhibited better dielectric properties ($\varepsilon_r = 8.4$ and $Q{\cdot}f_0 = 12{,}400$ GHz) when sintered at 950 °C. $ZnO–B_2O_3$ glass can be used as matrix component. Wu and Huang [10] provided the $ZnO–B_2O_3$ glass data, including density, dielectric properties, CTE, glass transformation (T_g)

* Corresponding author. Tel.: +86 27 87558482; fax: +86 27 87545167.
E-mail address: hyx@mail.hust.edu.cn (Y.-X. Hu).

0272-8842/$36.00
doi:10.1016/j.ceramint.2011.03.033

and softening points (T_s). Effects of $3ZnO–2B_2O_3$ (3Z2B) glass addition on densification and microwave properties of $(Ca_{1-x}Nd_{2x/3})TiO_3$ have been investigated by Wei and Jean [11]. However, no literature reports LTCC compositions of 3Z2B glass filled with alumina ceramic powder.

In the present paper, 3Z2B glass–Al_2O_3 composites were prepared for the first time as a novel potential candidate for the LTCC applications. The major concern of this paper was to examine the effects of glass content and sintering temperature on densification, crystallization, and microwave dielectric properties of 3Z2B glass–Al_2O_3 composites.

2. Experimental

3Z2B glass was prepared by a quenching method. High purity powder of ZnO and H_3BO_3 was weighed according to the nominal composition of $3ZnO–2B_2O_3$ and well mixed under a dry condition. The mixture was melted above 1150 °C using an alumina crucible, and quenched in water. The resulting frit was clear and no crystalline phase was detected by X-ray diffraction (XRD). The deformation temperature of the 3Z2B glass was measured by differential thermal analysis (Diamond TG/DTA, PerkinElmer Instruments). The frit was ground with deionized water and zirconia media using a planetary ball mill for 3 h. The resulting glass powder had a medium size of 5 μm. No difference in properties of 3Z2B glass–alumina composites is observed using two kinds of starting glass powder melted in an alumina crucible and a Pt crucible, respectively.

The 3Z2B glass powder with different amounts of α-Al_2O_3 (purity 99.8%, medium size 3 μm) powder was mixed in deionized water with zirconia media by a planetary mill for 1 h. The mixtures were dried, pelleted, and bilaterally pressed at about 110 MPa to make disk type samples with dimensions of 25 mm in diameter and 14–18 mm in height. Samples were then sintered in air at 600–950 °C for 2 h.

Crystalline phases of the sintered samples were identified with a diffractometer (*D*/Max-IIIA, Rigaku) using a Cu Kα target within 2θ range of between 10 and 80°. Sintering densities were measured by the Archimedes method. For differential thermal analysis (DTA) experiments, the samples were fired at a heating rate of 5 °C/min in flowing air. The microstructures of sintered compacts were observed from surfaces by scanning electron microscopy (SEM, Quanta 200).

The ε_r and $Q{\cdot}f_0$ values were determined using a silver cavity ca. 4 times the diameter of the test resonator (this ensured an isolated but shielded resonator) and an Advantest network analyzer (R3767C) operating in the $TE_{01\delta}$ resonance mode in reflectance [12,13]. For the measurement of τ_f, the technique is the same as that of $Q{\cdot}f_0$ measurement. The test cavity was placed over a thermostat and the temperature range used was from 30 to 80 °C. The τ_f values were calculated as follows:

$$\tau_f = \frac{(f_{80} - f_{30}) \times 10^6}{50 f_{30}} (\text{ppm/°C}) \quad (1)$$

where f_{80} and f_{30} are the resonant frequencies at 80 and 30 °C, respectively.

3. Results and discussion

3.1. Microstructure evolution of composites

Fig. 1 shows XRD patterns of 70 wt% glass–30 wt% Al_2O_3 composites sintered at 750–900 °C for 2 h. The XRD pattern of the sample sintered at 750 °C revealed that crystalline phases in this sample mainly consisted of Al_2O_3, $ZnAl_2O_4$, $3ZnO{\cdot}B_2O_3$, and $4ZnO{\cdot}3B_2O_3$, and that $ZnAl_2O_4$, $3ZnO{\cdot}B_2O_3$, and $4ZnO{\cdot}3B_2O_3$ phases formed below 750 °C. As the sintering temperature rose up to 800 °C, the Al_2O_3 and $3ZnO{\cdot}B_2O_3$ phases almost disappeared, and meanwhile $ZnAl_2O_4$ and $4ZnO{\cdot}3B_2O_3$ phases developed dramatically. At higher sintering temperature (850–900 °C) the crystalline phase composition of composites almost remained unchanged compared to that of the composite sintered at 800 °C. Similarly, it was reported by Yoon et al. [14] that $ZnAl_2O_4$ phase formed at 700 °C in a zinc borosilicate (ZBS) glass–Al_2O_3 composite system. In contrast no $4ZnO{\cdot}3B_2O_3$ phase was detected in that system.

The proportion of the phase constituents was quantitatively analyzed on a 70 wt% 3Z2B glass–30 wt% Al_2O_3 composite sample sintered at 900 °C using the *K* value method [15]. Since no crystalline Al_2O_3 was detected in this sample (Fig. 1, 900 °C), α-Al_2O_3 powders was taken as internal standard substance. The contents of crystalline $ZnAl_2O_4$ and $4ZnO{\cdot}3B_2O_3$ in this composite were measured to be 50.2 and 31.1 wt%, respectively, and the balance of 18.7 wt% might be assigned to the content of the residual glass phase.

The proportion of these three phases in this composite can also be calculated using starting material composition data according to the mass conservation. Suppose that Al_2O_3 was absent in the residual glass phase, and notice that no crystalline Al_2O_3 phase existed in the composite (Fig. 1, 900 °C). It is inferred that Al_2O_3 completely converted into $ZnAl_2O_4$, and therefore the content of $ZnAl_2O_4$ phase is calculated to be 53.9 wt%. This value is close to the one (50.2 wt%) obtained by the XRD quantitative analysis. Suppose further that ZnO completely converted into both $ZnAl_2O_4$ and $4ZnO{\cdot}3B_2O_3$ (i.e. ZnO was absent in the residual glass). The content of $4ZnO{\cdot}3B_2O_3$ is calculated to be 33.8 wt%, and close to the

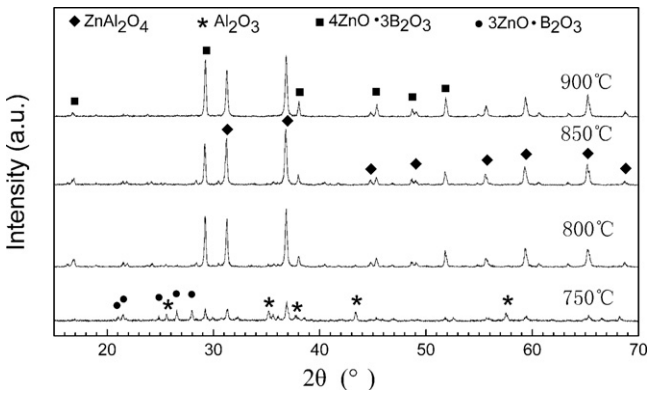

Fig. 1. Powder XRD patterns of 70 wt% glass–30 wt% Al_2O_3 composites sintered at 750–900 °C for 2 h.

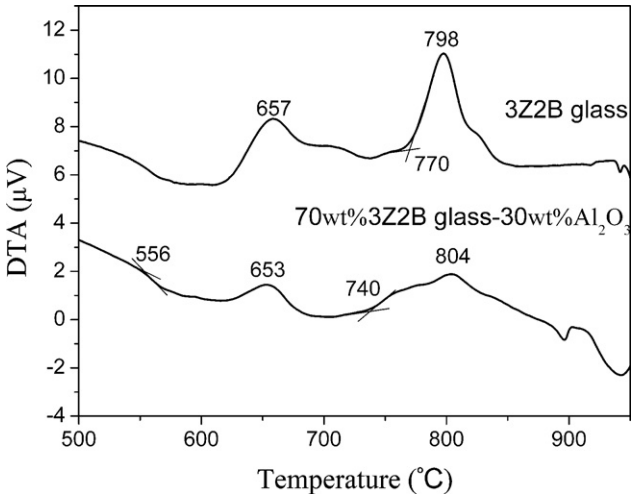

Fig. 2. DTA curves of the pure 3Z2B glass and the 70 wt% 3Z2B glass–30 wt% Al_2O_3 composite.

measured value (31.1 wt%) by the XRD quantitative analysis. Furthermore, the comparison between the measured values and the calculated ones shows that the residual glass phase contained only little amount of Al_2O_3 and ZnO, in other words, the residual glass phase was B-rich and Al- and Zn-poor.

Fig. 2 shows the DTA curves for a pure 3Z2B glass and a 70 wt% glass–30 wt% Al_2O_3 composite sample. The 3Z2B glass sample exhibited three main thermal events in the range of 400–900 °C. The weak endothermic peak located at 556 °C may correspond to the deformation temperature of 3Z2B glass and is close to the value reported by Wei and Jean [11]. The two exothermal peaks at 657 and 798 °C may be related to the formation of the crystalline $3ZnO{\cdot}B_2O_3$ and $4ZnO{\cdot}3B_2O_3$, respectively, in comparison with the XRD results in Fig. 1. Similarly, for the 70 wt% glass–30 wt% Al_2O_3 sample, the three peaks at 556, 653, and 804 °C are related to the deformation of 3Z2B glass and the formation of the crystalline $3ZnO{\cdot}B_2O_3$ and $4ZnO{\cdot}3B_2O_3$, respectively, indicating the addition of 30 wt% Al_2O_3 to the 3Z2B glass has no or little influence on these three events. The exothermal peak initiating at 740 °C may be due to the formation of the $ZnAl_2O_4$ spinel in comparison with the XRD results in Fig. 1.Fig. 3 shows SEM images of 70 wt% 3Z2B glass–30 wt% Al_2O_3 composites sintered at different temperatures. Big separate lumps with few small grain inclusions and a large amount of pores were observed in composites sintered at 700 °C (Fig. 3(a)). These lumps resulted from the softening and coalescence of glass particles. At 800 °C big glass lumps coalesced further to form a continuous phase, grains crystallized in the glass matrix, and the size and the number of pores decreased (Fig. 3(b)). At 850 °C the glass phase formed a completely continuous phase and encapsulated all crystalline grains, and less pores left (Fig. 3(c)). At 900 °C crystalline grains with an average size of ca. 400 nm formed fully, and glass phase content dramatically decreased (Fig. 3(d)). Furthermore some cubes and few slabs were observed in 900 °C samples. The elemental composition

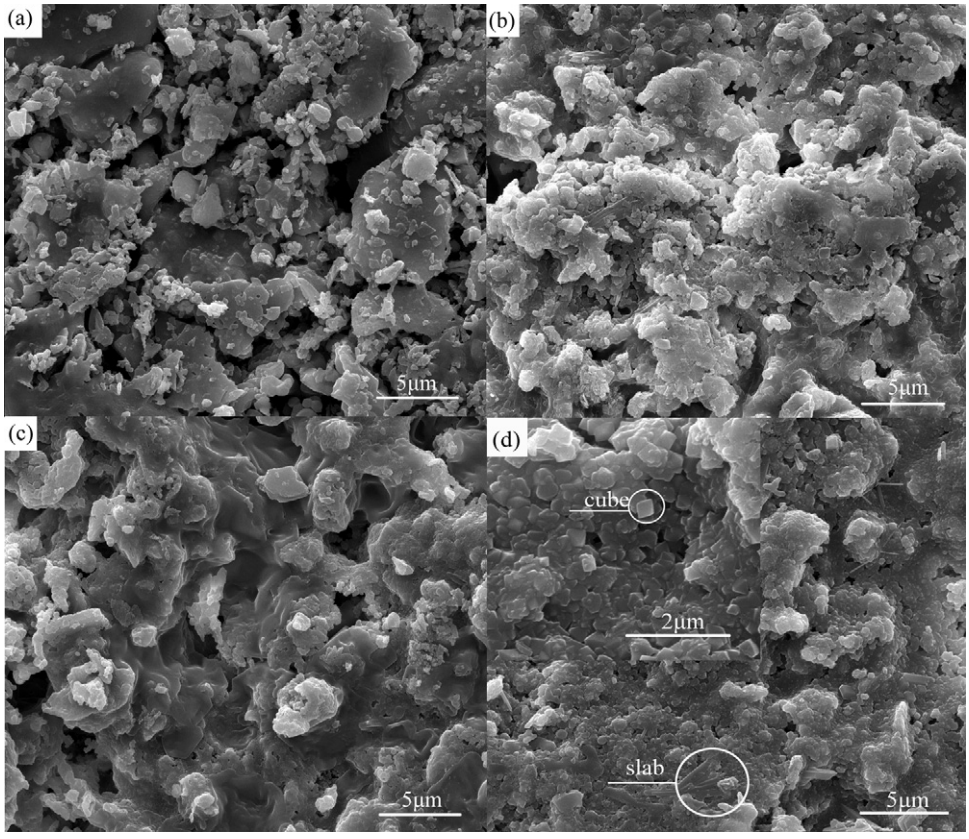

Fig. 3. Surface SEM images of 70 wt% 3Z2B glass–30 wt%Al_2O_3 composites sintered at (a) 700, (b) 800, (c) 850, and (d) 900 °C.

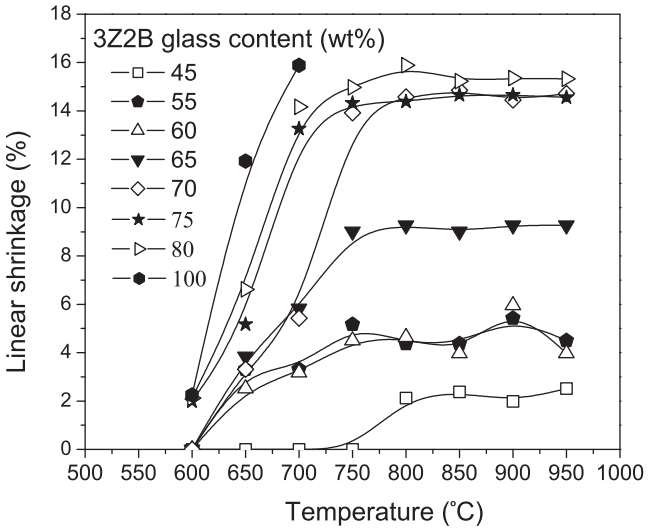

Fig. 4. Linear sintering shrinkage as a function of sintering temperature for composites with different 3Z2B glass contents.

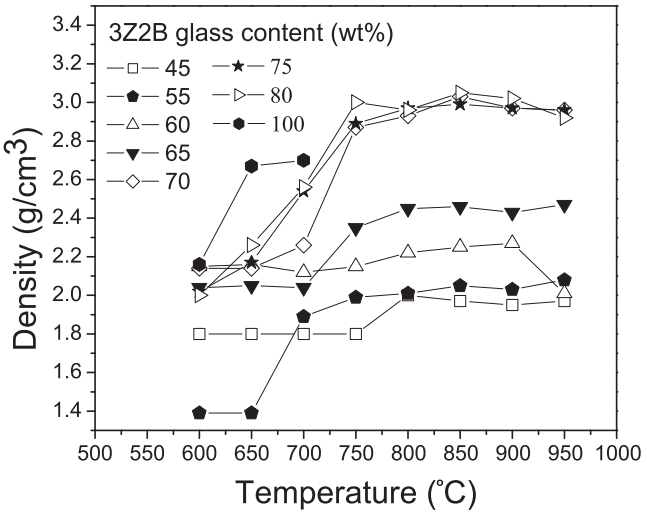

Fig. 5. Density as a function of sintering temperature for composites with different 3Z2B glass contents.

analysis of these phases with an energy dispersive spectrometer (EDS) was not carried out as the boron element of small atomic number cannot be detected. Nevertheless, in comparison with the XRD results in Fig. 1 these cubes are tentatively assigned to the $ZnAl_2O_4$ spinel phase and $4ZnO{\cdot}3B_2O_3$ phase since both of them are of cubic structure. The slabs may be assigned to the remnant $3ZnO{\cdot}B_2O_3$ phase since it is monoclinic.

Fig. 4 shows the linear sintering shrinkage behavior of 3Z2B–Al_2O_3 composites with different 3Z2B glass content sintered at 600–950 °C for 2 h. These composites exhibited one-stage densification behavior. Sintering shrinkage was limited to 2% at 600 °C due to the low sintering temperature, increased steeply in the temperature region of 600–800 °C, and reached a plateau in the second temperature region (800–950 °C) for most of composites. Furthermore, the maximal sintering shrinkage of composites increased with the increasing glass content. Composites showed a relatively small shrinkage (<5%) as glass content is less than 60 wt%, whereas a large shrinkage when the glass content is more than 65 wt%.

Fig. 5 summarizes the density results for composite samples with different 3Z2B glass content sintered at 600–950 °C for 2 h. The results are almost consistent with the tendency of sintering shrinkage. It is obvious that glass content and sintering temperature are two important factors in the densification process of composites. It is worthwhile pointing out that in the second temperature region the density of composites increased with the increasing glass content when glass content is no more than 70 wt%. Ink tests on the top surfaces of the composites sintered at 800–950 °C showed that composites were porous as glass content is no more than

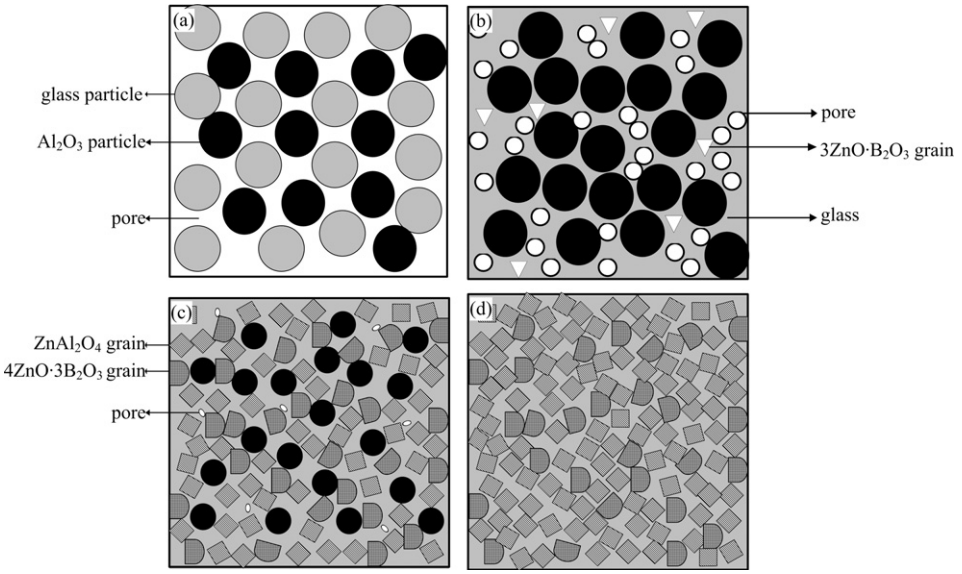

Fig. 6. Schematic of the densification and microstructure evolution of 3Z2B glass–Al_2O_3 composites during sintering: (a) green body, (b) softening of glass and particle rearrangement, (c) solution-precipitation, and (d) sintered body.

65 wt%, and turned dense as glass content is higher than 70 wt%. This result suggests that at least 70 wt% of glass content be needed to fill the pore in the green body.

Based on the above-mentioned XRD, DTA, SEM, sintering shrinkage, and density results, the following densification mechanism is proposed for 3Z2B glass–Al_2O_3 composites and illustrated schematically in Fig. 6. Firstly, below 556 °C, the composite remains green body status and consists of 3Z2B glass particles, α-Al_2O_3 particles, and pores (Fig. 6(a)). Secondly, 3Z2B glass begins to soften above 556 °C, and causes attractive forces between the solid particles, which leads to particle rearrangement and therefore to an increase in shrinkage (Fig. 6(b)) [16]. Obviously, the particle rearrangement is one of the factors which cause the steep increase in shrinkage during 600–800 °C.

Thirdly, dissolution of Al_2O_3 into the glass matrix and crystallization of the spinel and $4ZnO{\cdot}3B_2O_3$ phase from the glass matrix occur above 740 °C (Fig. 6(c)). Our observation that a clear 3Z2B glass liquid can be easily obtained by melting a mixture of ZnO and H_3BO_3 in the presence of 5 wt% Al_2O_3 implies that Al_2O_3 can dissolute in 3Z2B glass liquid at high temperature. The spinel phase may crystallize from glass liquid when Al_2O_3 content in glass liquid reaches dissolution saturation, which is different from the result reported by Dai et al. [17] that anorthite-type crystalline phases formed on the surface of Al_2O_3 particles during the sintering of Motorola T2000 dielectric.

The $4ZnO{\cdot}3B_2O_3$ phase may crystallize from glass liquid when the sintering temperature is high enough. So the solution-precipitation is the other one of the factors that causes the steep increase of shrinkage between 600 and 800 °C.

Fourthly, after the steep increase in shrinkage, solid-state sintering may take place. However, it is weak, and the shrinkage stays on the plateau. The sintered body is composed of $ZnAl_2O_4$ grains, $4ZnO{\cdot}3B_2O_3$ grains and residual glass phase (Fig. 6(d)). The end stage of the diverse composites may be different. For composites with low glass content, the densification may stop at the solution-precipitation stage due to the lack of glass phase. As a result, some alumina may exist in the sintered body besides the above three phases.

3.2. Microwave dielectric properties of composites

The dielectric properties of the 70 wt% 3Z2B glass–30 wt% Al_2O_3 composite sintered at 750–950 °C are summarized in Table 1. The dielectric constant was around 5.0 and did almost not vary with the sintering temperature in the range of 750–950 °C. However the sintering temperature had a great influence on the quality factor of the composite. The $Q{\cdot}f_o$ value of the composite was lower (<2000 GHz) at lower sintering temperature (750–800 °C), which may be due to the presence of a big volume fraction of pore and residual glass phase in composites at lower sintering temperature. While the $Q{\cdot}f_o$ value reached a plateau of ca. 8000 GHz at higher sintering temperature (850–950 °C), which is due to the complete densification and crystallization, and therefore less residual pores and glass in composites (Fig. 3). The τ_f value of the composite was −42.4 ppm/°C at lower sintering temperature (750 °C) and changed to and stayed at ca. −32 ppm/°C at higher sintering temperature (800–950 °C). This change in τ_f may result from the reduction of Al_2O_3 and glass phase and the formation of $ZnAl_2O_4$ and $4ZnO{\cdot}3B_2O_3$ at 800–950 °C. The τ_f value needs to be adjusted to near zero further [17–19]. Finally, it is worth to stress that the 70 wt% 3Z2B glass–30 wt% Al_2O_3 composite exhibited good and same microwave dielectric properties when sintered at 850–950 °C, and that this wide sintering temperature span (100 °C) is very conducive to the industrial production of the 70 wt% 3Z2B glass–30 wt% Al_2O_3 composite.

The good microwave dielectric properties of the 70 wt% 3Z2B glass–30 wt% Al_2O_3 composites sintered at 900 °C may attribute to the high content of $ZnAl_2O_4$ and $4ZnO{\cdot}3B_2O_3$ in the composites. The XRD quantitative analysis shows the total content of these two phases is 81.3 wt%. $ZnAl_2O_4$ is of good microwave dielectric properties of $\varepsilon_r = 8.5$, $Q{\cdot}f_0 = 56{,}300$ GHz, and $\tau_f = -79$ ppm/°C [20], while for $4ZnO{\cdot}3B_2O_3$ these property data which are useful for our discussion have not been reported so far. Based on the above-mentioned dielectric properties of the 70 wt%3Z2B glass–30 wt% Al_2O_3 composites, at least one of the residual glass phase and $4ZnO{\cdot}3B_2O_3$ phase is with low dielectric constant ($\varepsilon_r < 5$) while $4ZnO{\cdot}3B_2O_3$ phase might have high $Q{\cdot}f_0$ due to its large content (31.1 wt%) in the composites. The presence of a great amount of these two crystalline phases with high $Q{\cdot}f_0$ in the composites improves dramatically the $Q{\cdot}f_0$ of the composites.

Table 2 gives the microwave dielectric properties of composites with different glass content sintered at 900 °C. The dielectric constant increased from 3.6 at 45 wt% of glass content to 5.5 at 65 wt% of glass content, and this is mainly due to the increase in the degree of densification of the composites. The dielectric constant varied slightly with the glass content in the range of 70–80 wt%, and this mainly results from the differences of dielectric constant and content of each phase in composites.

Table 1
Microwave dielectric properties of 70 wt% 3Z2B glass–30 wt% Al_2O_3 composites sintered at 750–950 °C.

	Sintering temperature (°C)				
	750	800	850	900	950
Dielectric constant, ε_r	5.3	5.0	4.9	5.0	4.8
Resonant frequency (GHz)	7.1	7.7	7.5	7.1	7.6
Q	260	260	1100	1170	980
$Q{\cdot}f_0$ (GHz)	1487	2000	8809	8689	7935
τ_f (ppm/°C)	−42.4	−32.7	−31.8	−32.7	−32.4

Table 2
Microwave dielectric properties of 3Z2B glass–Al_2O_3 composites with different glass content sintered at 900 °C.

	Glass content (wt%)						
	45	55	60	65	70	75	80
Dielectric constant	3.6	3.6	3.9	5.5	5.0	4.9	5.5
Resonant frequency (GHz)	7.3	7.3	7.3	7.5	7.1	7.7	7.0
Q	630	630	720	760	1170	610	500
$Q{\cdot}f_0$ (GHz)	4204	4247	5119	6087	8689	4812	3483

The $Q{\cdot}f_0$ values exhibited maximum at glass content of 70 wt%. The main reason why the composites with lower glass content (<65 wt%) were of lower $Q{\cdot}f_0$ values is probably due to the lack of densification in the composites. Higher glass content (>75 wt%) led to poor $Q{\cdot}f_0$ values of composites for the sake of presence of the excess residual glass phase.

4. Conclusions

This preliminary work concludes that the microwave dielectric properties of newly suggested LTCC compositions, which are based on 3Z2B glass matrix and Al_2O_3 filler, are sensitive to the glass content and sintering temperature. The densification mechanism for 3Z2B–Al_2O_3 composites was reported. The linear shrinkage of 3Z2B glass–Al_2O_3 composites showed a steep increase below 800 °C and a plateau behavior between 800 and 950 °C, indicating that one-stage densification occurred. A clear evidence of the involvement of new phases, such as $ZnAl_2O_4$, demonstrated that certain chemical reaction between the glass matrix and the alumina filler acted positively and resulted in an improvement in microwave dielectric properties of the composites. Meanwhile, the crystallization product such as $4ZnO{\cdot}3B_2O_3$ also played an important role in improving the microwave dielectric properties. The composition of 70 wt% 3Z2B glass and 30 wt% alumina could be densified at 850–950 °C and exhibited excellent microwave dielectric properties: $\varepsilon_r = \sim 5.0$, $Q{\cdot}f = \sim 8000$ GHz, and $\tau_f = \sim$-32 ppm/°C at ~7.0 GHz. The wide sintering temperature span makes it possible the industrial production of the 70 wt% 3Z2B glass–30 wt% Al_2O_3 composite. The investigation of the application of this composition in LTCC is under way.

Acknowledgements

This work was supported by State Key Laboratory of Material Processing and Die & Mould Technology, Huazhong University of Science and Technology.

References

[1] M.T. Sebastian, H. Jantunen, Low loss dielectric materials for LTCC applications: a review, Int. Mater. Rev. 53 (2008) 57–90.
[2] Y.P. Guo, H. Oshato, K. Kakimoto, Characterization and dielectric behavior of willemite and TiO_2-doped willemite ceramics at millimeter-wave frequency, J. Eur. Ceram. Soc. 26 (2006) 1827–1830.
[3] C.S. Chen, C.C. Chou, C.S. Chen, I.N. Lin, Microwave dielectric properties of glass–ceramic composites for low temperature co-firable ceramics, J. Eur. Ceram. Soc. 24 (2004) 129–134.
[4] M.M. Krzmanc, M. Valant, D. Suvorov, A structural and dielectric characterization of $Na_xCa_{1-x}Al_{2-x}Si_{2+x}O_8$ ($x = 0$ and 1) ceramics, J. Eur. Ceram. Soc. 25 (2005) 2835–2838.
[5] O. Dernovsek, A. Naeini, G. Preu, W. Wersing, M. Eberstein, W.A. Schiller, LTCC glass–ceramic composites for microwave application, J. Eur. Ceram. Soc. 21 (2001) 1693–1697.
[6] M. Kono, H. Takagi, T. Tatekawa, H. Tamura, High Q dielectric resonator material with low dielectric constant for millimeter-wave applications, J. Eur. Ceram. Soc. 26 (2006) 1909–1912.
[7] A. Stiegelschmitt, A. Roosen, C. Ziegler, S. Martius, L.P. Schmidt, Dielectric data of ceramic substrates at high frequencies, J. Eur. Ceram. Soc. 24 (2004) 1463–1466.
[8] H. Ohsato, T. Tsunooka, A. Kan, Y. Ohishi, Y. Miyauchi, Y. Tohdo, et al., Microwave-millimeterwave dielectric materials, Key Eng. Mater. 26 (2004) 195–198.
[9] Y.J. Seo, D.J. Shin, Y.S. Cho, Phase evolution and microwave dielectric properties of lanthanum borate-based low-temperature co-fired ceramics materials, J. Am. Ceram. Soc. 89 (2006) 2352–2355.
[10] J.M. Wu, H.L. Huang, Microwave properties of zinc, barium and lead borosilicate glasses, J. Non-Cryst. Solids 260 (1999) 116–124.
[11] C.H. Wei, J.H. Jean, Low-fire processing of $(Ca_{1-x}Nd_{2x/3})TiO_3$ microwave ceramics, J. Am. Ceram. Soc. 86 (2003) 93–98.
[12] B.W. Hakki, P.D. Coleman, A dielectric resonator method of measuring inductive capacities in the millimeter range, IEEE Trans. Micro. Theory Technol. 8 (1960) 402–410.
[13] W.E. Courtney, Analysis and evaluation of a method of measuring the complex permittivity and permeability microwave insulators, IEEE Trans. Microw. Theory Technol. 18 (1970) 476–485.
[14] S.O. Yoon, S.H. Shim, K.S. Kim, J.G. Park, S. Kim, Low-temperature preparation and microwave dielectric properties of ZBS glass–Al_2O_3 composites, Ceram. Int. 35 (2009) 1271–1275.
[15] F.H. Chung, Quantitative interpretation of X-ray diffraction patterns of mixtures. II. Adiabatic principle of X-ray diffraction analysis of mixtures, J. Appl. Crystallogr. 7 (1974) 519–525.
[16] S. Kemethmuller, M. Hagymasi, A. Stiegelschmitt, A. Roosen, Viscous flow as the driving force for the densification of low-temperature co-fired ceramics, J. Am. Ceram. Soc. 90 (2007) 64–70.
[17] S.X. Dai, R.F. Huang Sr., D.L. Wilcox, Use of titanates to achieve a temperature-stable low-temperature cofired ceramic dielectric for wireless applications, J. Am. Ceram. Soc. 85 (2002) 828–832.
[18] D.L. Wilcox Sr, R.F. Huang, S. Dai, Enabling materials for wireless multilayer ceramic integrated circuit (MCIC) application, in: Ceramic Transaction, Multilayer Electronic Ceramic Devices, Am. Ceram. Soc, Westerville, OH, USA, (1998), pp. 201–213.
[19] S. Dai, R.F. Huang Sr., D.L. Wilcox, Proc. Temperature Stable, Low Loss and Low Fire Dielectric for Consumer Wireless Applications, 1st China Int. Conf. on High Performance Ceramics, Beijing, China, 1998.
[20] P.K. Surendran, M.T. Sebastian, M.V. Manjusha, J. Philip, A low loss, dielectric substrate in $ZnAl_2O_4$–TiO_2 system for microelectronic applications, J. Appl. Phys. 98 (2005) 044101.